Plasma-Derived Small Extracellular Vesicles From VKH Patients Suppress T Cell Proliferation Via MicroRNA-410-3p Modulation of CXCL5 Axis

Bing Li,[1] Nan Sun,[1] Fuhua Yang,[1] Kailei Guo,[1] Lingzi Wu,[1] Mingming Ma,[1] Hui Shao,[2] Xiaorong Li,[1] and Xiaomin Zhang[1]

[1]Tianjin Key Laboratory of Retinal Functions and Diseases, Tianjin Branch of National Clinical Research Center for Ocular Disease, Eye Institute and School of Optometry, Tianjin Medical University Eye Hospital, Tianjin, China
[2]Department of Ophthalmology and Visual Sciences, Kentucky Lions Eye Center, University of Louisville, School of Medicine, Louisville, KY, United States

Correspondence: Xiaomin Zhang, Tianjin Key Laboratory of Retinal Functions and Diseases, Tianjin Branch of National Clinical Research Center for Ocular Disease, Eye Institute and School of Optometry, Tianjin Medical University Eye Hospital, Tianjin, China; xzhang08@tmu.edu.cn.

BL and NS contributed equally to this work.

Received: February 6, 2023
Accepted: August 9, 2023
Published: September 6, 2023

Citation: Li B, Sun N, Yang F, et al. Plasma-derived small extracellular vesicles from VKH patients suppress T cell proliferation via MicroRNA-410-3p modulation of CXCL5 axis. *Invest Ophthalmol Vis Sci.* 2023;64(12):11. https://doi.org/10.1167/iovs.64.12.11

Purpose. Circulating exosomes regulate immune responses and induce immune tolerance in immune-mediated diseases. This study aimed to investigate the role of circulating small extracellular vesicles (sEVs) derived from patients with Vogt-Koyanagi-Harada (VKH) syndrome, in T-cell responses.

Methods. The sEVs were isolated from the plasma of healthy controls, patients with VKH, and other uveitis patients. The effects of autologous and allogeneic sEVs on the proliferation of circulating $CD4^+$ T cells were evaluated. Microarray analysis of sEVs was performed to determine their differential miRNA expression profiles. The target genes of the candidate miRNA were predicted and verified. The role of both the candidate miRNA and target genes in T-cell proliferation was tested.

Results. Plasma-derived sEVs from patients with VKH inhibited the proliferation of autologous $CD4^+$ T cells. Among all the miRNAs that might be associated with inflammatory activity, we found that miR-410-3p had the largest number of T-cell proliferation target genes. MiR-410-3p mimics inhibited the proliferation of Jurkat cells and $CD4^+$ T cells. C-X-C motif chemokine ligand 5 (CXCL5) was confirmed to be a potential target gene of miR-410-3p, and siRNA-mediated CXCL5 knockdown inhibited cell proliferation.

Conclusions. Circulating sEVs exert an inhibitory effect on autologous $CD4^+$ T cells mediated by miR-410-3p by targeting CXCL5, supporting the possibility of using autogenic sEVs to inhibit ocular inflammation.

Keywords: CXCL5, exosomes, miR-410-3p, small extracellular vesicles, Vogt-Koyanagi-Harada

Vogt-Koyanagi-Harada (VKH) syndrome, a systemic noninfectious inflammatory disorder accompanied by bilateral granulomatous panuveitis, often leads to severely low visual acuity and blindness without treatment.[1] The etiology and pathogenesis of VKH are not clear, but current research has shown they may be related to aberrant immune reactivity, genetic susceptibility, and viral infection.[2–4] Early and appropriate treatment using systemic corticosteroids, immunosuppressants, and biological agents is the mainstay therapy for patients with VKH.[5] However, these long-term therapies result in adverse effects, including abnormalities in lipid and glucose metabolism, serious infection, impairment of hepatic and renal function, and potential oncogenesis.[6] Therefore it is essential to find novel therapeutic approaches for VKH.

Extracellular vesicles (EVs) are cell-derived vesicles enclosed by a lipid bilayer, ranging from 30 nm to 1000 nm in diameter,[7] which includes exosomes, microvesicles, and apoptotic bodies. Exosomes, between 30 and 150 nm across, are enriched in RNAs, proteins, and lipids. Exosomes mediate intercellular communication[8] and play key roles in the regulation of physiological processes,[9–11] and the development of disease pathogenesis.[12] Exosomes can induce or suppress immune responses in diseases.[13,14] Vaccination with exosomes isolated from the plasma of rats with uveitogenic antigen-induced uveitis reduced the severity of the disease in an antigen-specific manner, and have been indicated as a therapy for autoimmune uveitis.[15] Because circulating exosomes contain autoantigens that may regulate immune responsiveness,[16] it was postulated that exosomes exert therapeutic effects by inducing autoantigen-based immune tolerance.[15] The establishment and maintenance of immune tolerance are associated with the deletion or anergy of effector T cells[17,18] and induction of T regulatory cells (Tregs).[19] The immunosuppressive microenvironment is important for the successful induction of immune tolerance.[20]

In this study, we aimed to clarify the role of exosomes in the pathological process of VKH disease and the possible mechanism by which exosomes induce immune tolerance.

We investigated the effect of plasma exosomes from patients with VKH on autologous T cells and the role of miRNAs encapsulated in exosomes. Because it is difficult to obtain pure exosome samples using current separation approaches, the term small extracellular vesicles (sEVs) was used instead, as suggested by the new minimal information for studies of extracellular vesicle guidelines.[21] We found that plasma-derived sEVs from patients with VKH reduced the proliferation of autologous $CD4^+$ T cells, and upregulated miR-410-3p in sEVs may mediate the suppressive effect by inhibiting CXCL5 expression.

Material and Methods

Human Sample Group and Collection

Ethics approval was obtained from the Tianjin Medical University Eye Hospital Ethics Committee (No. 2016KY-14). All patients and healthy volunteers provided informed consent. The diagnosis of VKH was made according to Yang et al.[22] Patients were grouped as healthy individuals (normal controls [NC]), acute inflammation stage of VKH with duration of less than two weeks (AST), unstable recovery stage of VKH less than three month of treatment, with symptomatic improvement but not complete resolution (UST), and stable stage of disease over three months of treatment (SST).[23] Peripheral blood was obtained from NC and patients with VKH or other types of uveitis (including Behçet's disease uveitis and idiopathic panuveitis). The clinical information of the participants is listed in Supplementary Table S1. The patients with VKH in the AST and other uveitis patients were at active inflammation stage and had received no corticosteroids or immunosuppressants. The upper plasma was transferred and stored in the biobank at −80 °C until further processing.

Isolation and Purification of sEVs

The sEVs were purified from the plasma using ultracentrifugation as previously reported.[24] The samples were carefully defrosted on ice and 1 mL diluted in 10 mL PBS. The diluted samples underwent sequential centrifugation at 2000*g* for 15 minutes, followed by 10,000*g* for 30 minutes. The sEV pellets were precipitated by centrifugation at 110,000*g* for two hours. The pellets were resuspended in 11 mL cold PBS and spun in a centrifuge at 110,000*g* for two hours. The purified sEVs were collected in 50 µL of PBS.

Transmission Electron Microscopy (TEM)

The sEVs sample 20 µL (1 mg/mL) was placed onto copper grids and stained with 1% uranyl acetate (20 µL) for TEM observation (Hitachi HT7700; Hitachi, Tokyo, Japan).

Nanoparticle Tracking Analysis (NTA)

NTA was performed to analyze the size distribution of sample using NanoSight NS300 system (NanoSight, Malvern, UK). Particle-free water was added to dilute the sEVs suspension to 1 mL. NTA software (NTA 3.3 Dev Build 3.3.104) was used to analyze the results.[25]

Western Blot

Proteins from sEVs and cells were extracted using RIPA solution plus protease inhibitors. We measured protein concentration with a BCA protein assay kit (Solarbio Life Science, Beijing, China). The SDS-polyacrylamide gel electrophoresis was used for protein separation and then was transferred onto polyvinylidene difluoride membranes. Five percent skim milk was used to block the membranes before primary antibodies were added.

The primary antibodies included CD9 (1:2000; Abcam, Cambridge, MA, USA), CD63 (1:1000; Abcam), TSG101 (1:1000; Proteintech, Chicago, IL, USA), CXCL5 (1:2000; Abcam), and β-actin (1:5000; Cell Signaling Technology, Danvers, MA, USA). After three 10-minute washes with Tris-buffered saline with Tween 20, incubation with secondary antibodies (1:5000; Cell Signaling Technology) followed. The protein bands were detected by enhanced chemiluminescence and quantified by ImageJ software.

MiRNA Microarray Assay

Microarray analysis of plasma samples was performed to identify differentially expressed miRNAs (DEMs) in circulating sEVs isolated from patients and NC. In accordance with the manufacturer's protocol, sample labeling and microarray hybridization were finished. The arrays were scanned using a G2505C Scanner (Agilent Technologies, Santa Clara, CA, USA).

RNA Isolation and RT-PCR

Cell-free total RNA (including miRNA) from sEVs was purified using the miRNeasy Serum/Plasma Kit (Qiagen, Hilden, Germany) based on the manufacturer's protocol. The cDNA was obtained through reverse transcription using the miScript II RT Kit (Qiagen). Total RNA extraction from cells was performed using TRIzol Reagent (Invitrogen, Carlsbad, CA, USA) and reverse transcribed into cDNA using the Revertaid kit (Thermo Fisher Scientific, Waltham, MA, USA). RT-PCR was performed using an ABI 7900 fast (Applied Biosystems, Foster City, CA, USA). U6 and GAPDH were chosen as the internal references for miRNA and other molecules, respectively. Primers for miR-410-3p, U6, *GAPDH*, *USP25*, *CXCL5*, and *IFNAR1* are listed in Supplementary Table S2.

Target Gene Prediction and Pathway Analysis

The patterns of selected DEMs were obtained using the R package TCseq (v1.14.0).[26] Verified interactions between selected miRNAs and target genes were retrieved from the miRTarBase and TarBase databases using the R package multiMiR (v1.12.0).[27] Target genes of selected DEMs were subjected to gene ontology (GO) analysis, Kyoto Encyclopedia of Genes and Genomes (KEGG) pathway analysis, and Reactome enrichment analysis using the R packages clusterProfiler (v.3.18.1)[28] and ReactomePA (v.1.40.0).[29] The threshold for statistical significance was a Benjamini-Hochberg–adjusted P value ≤ 0.05. The results were visualized using the R package ggplot2 (v.3.3.3).[30]

Cell Culture and Transfection

Human peripheral blood mononuclear cells were obtained from blood samples using density gradient ultracentrifugation with a lymphocyte separation medium (Solarbio, China). $CD4^+$ T cells were sorted from peripheral blood mononuclear cells using a $CD4^+$ T Cell Isolation Kit and LS Column (Miltenyi Biotec, Bergisch Gladbach, Germany). Primary T cells were stained for 10 min at room

Investigative Ophthalmology & Visual Science

temperature with 2 µmol/L carboxyfluorescein diacetate succinimidyl ester (CFSE) (Thermo Fisher Scientific, MA, USA) in PBS and diluted to a concentration of 1×10^6 cells/mL. Immunocult human CD3/CD28 T cell activator (25 µL/mL, Stemcell Technologies, Vancouver, BC, Canada) was added to the cell suspension to stimulate T cells, and the cell suspension was seeded in 96-well plates (200 µL/well).

In each proliferation assays, one VKH patient in the AST was involved to obtain $CD4^+$ T cells, whose plasma was purified to obtain autologous sEVs (Auto-sEVs). Allogeneic sEVs (Allo-sEVs) and healthy controls' sEVs (HC-sEVs) were obtained from other uveitis patients and HC, respectively. $CD4^+$ T cells were cultured with different sEVs (10 µg).

Jurkat cells were seeded in 96-well plates at 4×10^4 cells per well in 100 µL culture medium and transfected with miRNA mimics (100 nM), inhibitor (300 nM), or siRNA (100 nM, GenePharma, Nanjing, China) using Lipofectamine 3000 (Invitrogen). $CD4^+$ T cell were transfected with mimics at the final concentration of 100 nM.

Cell Proliferation Assay

Cell viability and proliferation were detected after 24, 48, and 72 hours of treatment using a Cell Counting Kit-8 (CCK-8) (Dojindo Molecular Technologies, Kumamoto, Japan). Optical density (OD_{450}) was detected using a microplate reader (Infinite 200 Pro; Tecan, Männedorf, Switzerland).

Flow Cytometry Assay

Flow cytometry was chosen to assess the purity of $CD4^+$ T cells used for subsequent experiments. For the cell proliferation experiments, T cells were stained with CFSE before being seeded in 96-well plates and incubated for 96 h in the dark. T cells were collected and stained with Anti-CD4-APC antibody (dilution: 1:1000; Abcam) for 30 minutes. Cell proliferation was quantified by CFSE fluorescence using flow cytometry at 96 hours after treatment.

Similarly, apoptotic cells were analyzed using the FITC Annexin V Apoptosis Kit (KeyGEN BioTECH, China). The number of apoptotic cells, including both early and late apoptotic cells, was calculated.

Statistical Analysis

Data were analyzed using SPSS (IBM, Armonk, NY, USA), FlowJo (FlowJo, Ashland, OR, USA), and Prism software (GraphPad Software, San Diego, CA, USA). The normality and homogeneity of variance were calculated from the data. Non-normal data were log-transformed to meet the assumption of normality before analysis. An independent-sample *t*-test was performed to analyze data between two groups, and a one-way ANOVA was used for data analysis involving more than two groups, as appropriate. Statistical significance was considered as $P < 0.05$.

Results

Plasma-Derived sEVs From Patients With VKH Inhibited the Proliferation of Autologous $CD4^+$ T Cells

We purified sEVs from the plasma of healthy controls and patients with acute VKH or other types of uveitis with active inflammation, using ultracentrifugation. TEM showed that the sEVs were round or oval membranous vesicles (Fig. 1A). The mean diameter of sEVs was confirmed as 117.7 ± 60.0 nm by NTA (Fig. 1B). The conventional exosome markers CD63, CD9, and TSG101 were detected using Western blotting (Fig. 1C). $CD4^+$ T cells from acute patients with VKH were stimulated with Immunocult human CD3/CD28 T cell activator in the presence of PBS, HC-, Allo-, or Auto-sEVs for 96 hours. Notably, the frequency of $CD4^+$ T cells cultured with Auto-sEVs was significantly reduced compared to that in cells cultured with HC-sEVs and the control (Figs. 1D, 1E; $P < 0.05$). The percentage of apoptotic cells in the PBS, Allo-sEV, and Auto-sEV groups was detected by flow cytometry (Fig. 1F), and there was no significant difference in cell apoptosis among the three groups (Fig. 1G; $P > 0.05$). These results indicated that circulating sEVs from acute VKH can inhibit autologous T cell proliferation without affecting cell apoptosis.

DEMs Profile and the Correlation Between Selected miRNAs With T-Cell Proliferation in sEVs From Patients With VKH

To determine the mechanisms by which plasma VKH patient sEVs inhibit the proliferation of $CD4^+$ T cells, we analyzed the miRNA expression profiles of plasma sEVs from NC and patients with VKH at AST, UST, and SST. Different miRNA expression profiles were identified in the four groups (Fig. 2A). We identified 870 miRNAs in sEVs. Of these, 45.40% (395/870) had been previously recorded in the ExoCarta database (Fig. 2B). After the comparison of miRNAs in AST, UST, or SST versus NC, the numbers of upregulated and downregulated miRNAs were identified (Fig. 2C). To investigate changes in miRNA expression at different VKH stages, miRNA expression patterns were analyzed using the TCseq package. Two miRNA expression patterns (Figs. 2D, 2E) were identified that were associated with disease development. According to the screening criteria of fold change FC (AST vs. NC) < -2 (downregulated) and $|$FC (SST vs. NC)$|$ <2 (no change)), five miRNAs were significantly downregulated at AST in cluster1 (Fig. 2F). Forty-six miRNAs were upregulated at AST and UST in cluster2 (Fig. 2G) using the screening criteria of FC (AST vs. NC) > 2 (upregulated), FC (UST vs. NC) > 2 (upregulated), and $|$FC (SST vs. NC)$|$ <2 (no change).

To explore the potential function of the differentially expressed miRNAs, the target genes of the 46 upregulated miRNAs were identified using the miRTarBase and tarbase databases. Next, we performed GO, KEGG, and Reactome enrichment analysis of the target genes. The GO analysis identified that target genes were enriched for ubiquitin-like protein ligase binding, ribonucleoprotein granules, and regulation of mRNA metabolic processes (Fig. 2H). The enriched KEGG pathways for the target genes included the neurotrophin signaling pathway and Hepatitis B (Fig. 2I). The Reactome pathway was significantly enriched in oncogene-induced senescence, PTEN regulation, and PIP3-AKT signaling (Fig. 2J). It is well known that the activation of PI3K-AKT signaling can promote cell growth, proliferation, and survival.[31]

We sought to determine which sEV-derived miRNAs may be critical in inhibiting autologous $CD4^+$ T cell proliferation (Fig. 1E). Sixty-seven genes associated with T cell proliferation (Supplementary Excel S1) were found to interact with the 46 upregulated miRNAs. Target genes

Investigative Ophthalmology & Visual Science

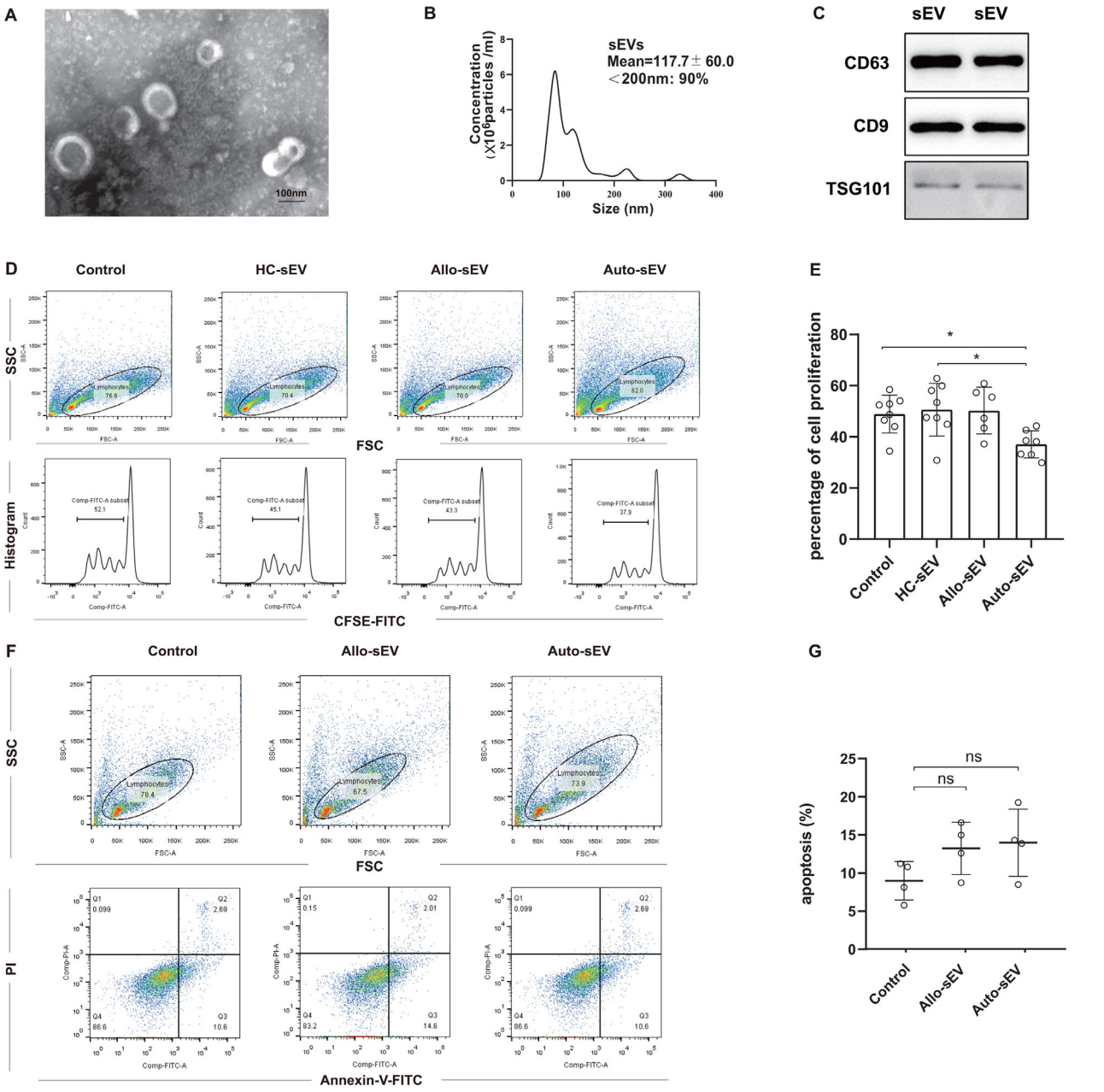

Figure 1. Circulating sEVs from patients with VKH selectively inhibited the proliferation of autologous $CD4^+$ T cells without affecting cell apoptosis. (**A**) The morphology of sEVs was observed using TEM (*scale bar:* 100 nm). (**B**) The size distribution of the sEVs was obtained through NTA. The mean size of sEVs was 117.7 ± 60.0 nm. (**C**) Exosome marker proteins (CD63, CD9, and TSG101) were identified using Western blotting. (**D**) Representative dot plot and histogram of flow cytometry data. Cell proliferation was quantified by measuring CFSE fluorescence using flow cytometry after 96 hours. (**E**) Percentage proliferation of T cells was assessed using flow cytometry. $CD4^+$ T cells were obtained from the peripheral blood of patients with VKH at the active stage and were cultured with PBS as the control ($n = 8$), HC-sEVs ($n = 8$), Allo-sEVs ($n = 6$), or Auto-sEVs ($n = 7$) under stimulation with human CD3/CD28 T cell activator for 96 h. (**F**) Representative dot plot of flow cytometry data. Annexin V-positive/PI-negative cells were regarded as apoptotic. (**G**) Histogram of the cell apoptosis rate detected by flow cytometry ($n = 4$). In E and G, each dot represents one patient and *n* represents the number of patients.

were searched in five databases (miRTarBase, TarBase, DIANA-microT, miRanda, and PITA) and used to match the proliferation gene list. We calculated the number of genes associated with T cell proliferation targeted by each miRNA and found that miR-410-3p had the largest number of T-cell proliferation target genes and might be crucial for inhibiting the proliferation of $CD4^+$ T cells (Fig. 2K).

MiR-410-3p Was Overexpressed in the sEVs From Acute Patients With VKH and Could Inhibit the Proliferation of Jurkat Cells and $CD4^+$ T Cells

We verified the changes in miR-410-3p levels in circulating sEVs by RT-PCR. The relative expression of miR-410-3p in AST was significantly higher than in the other three groups (Fig. 3A). To explore the possible role of miR-410-3p

Investigative Ophthalmology & Visual Science

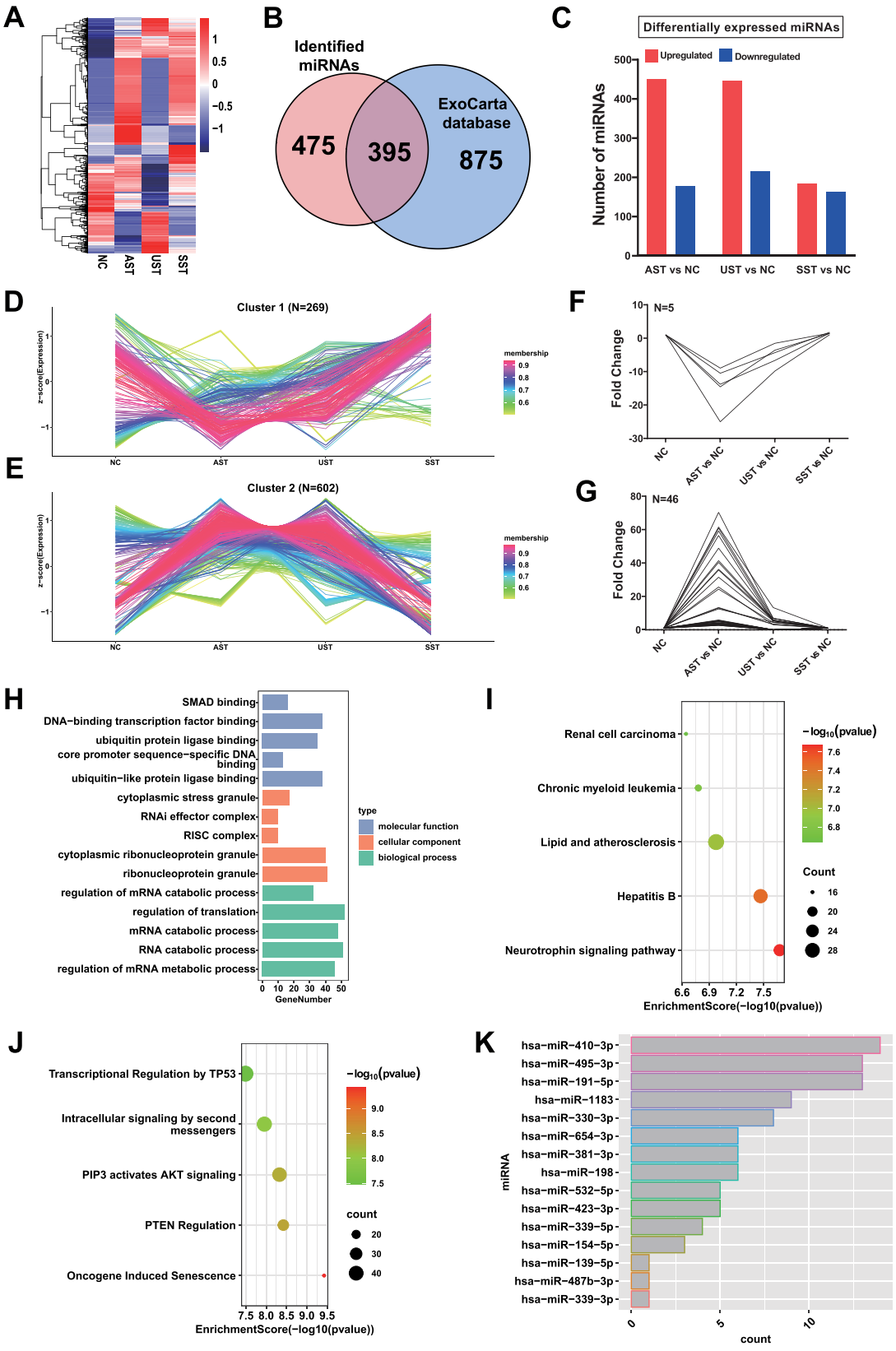

Figure 2. MiRNA profiling of sEVs from patients with VKH and NC, and GO and KEGG analysis for the targeted genes. (**A**) Heatmap of the DEMs in miRNA expression profiling in patients with VKH at different stages of disease compared to the NC. (**B**) Venn diagram of miRNAs overlap in the ExoCarta database. (**C**) Histogram of the number of DEMs in patients with VKH at different stage of disease versus control. (**D–G**) The two miRNAs expression patterns of NC and different stages of VKH conducted by cluster analysis. (**H**) GO analysis of miRNA target genes. Top five terms were displayed with three GO categories. (**I**) KEGG analysis of miRNA target genes. (**J**) Reactome analysis of miRNA target genes. (**K**) Number of genes associated with T cell proliferation targeted by each miRNA.

Investigative Ophthalmology & Visual Science

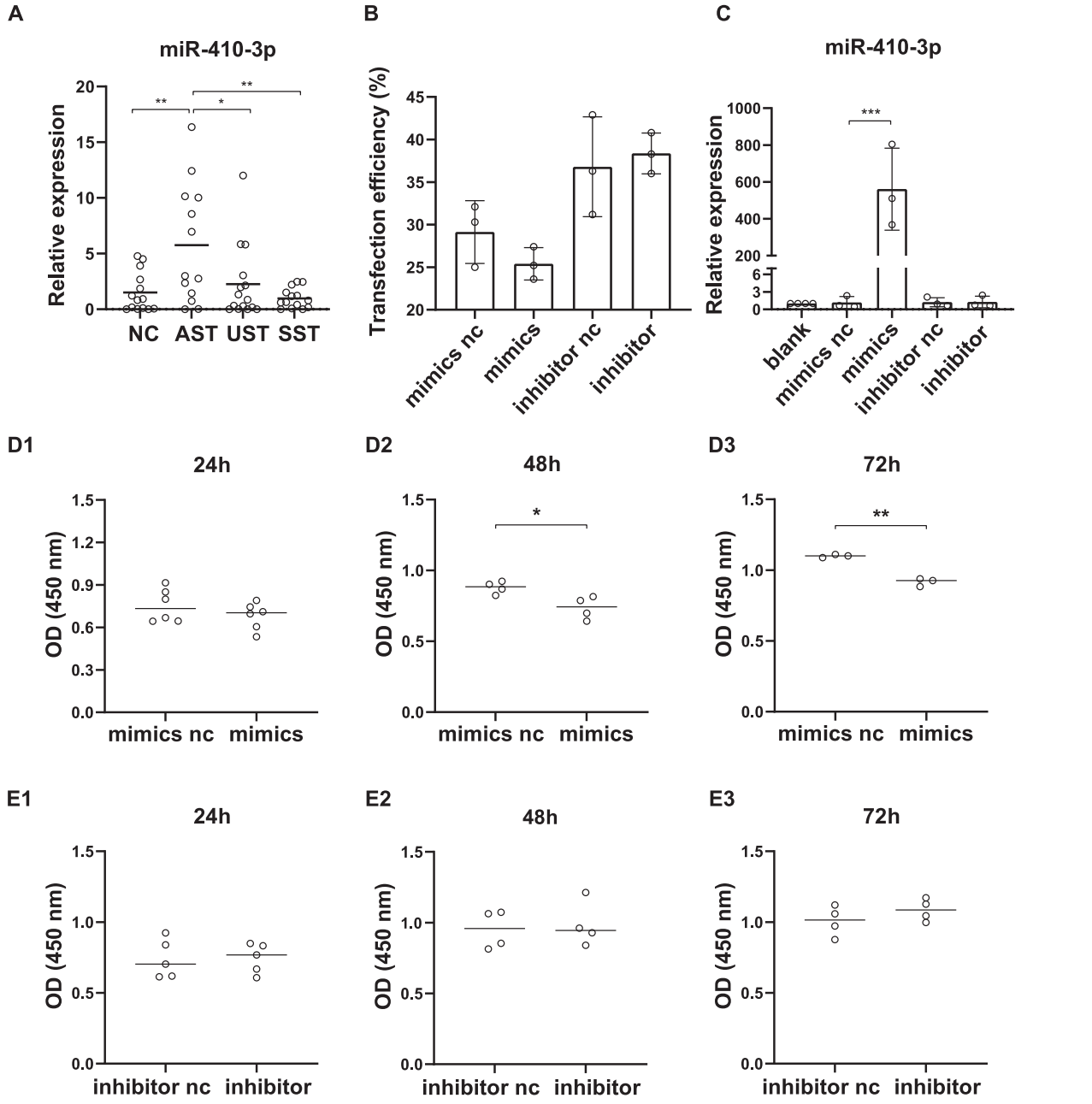

Figure 3. Expression levels of miR-410-3p and the function of miR-410-3p on Jurkat cells. (**A**) The relative expression of miR-410-3p in sEVs from patients with VKH and NC using RT-PCR. Each dot represents one patient. (**B**) Transfection efficiency of Jurkat cells post-transfected with miR-410-3p mimics or inhibitor ($n = 3$). (**C**) Relative expression of miR-410-3p in Jurkat cells post-transfected with miR-410-3p mimics or inhibitor or control using RT-PCR ($n = 3$). (**D1–D3**) The OD value at 450 nm of Jurkat cells post-transfected with miR-410-3p mimics or normal control for 24 h ($n = 5$), 48 h ($n = 4$), and 72 h ($n = 3$). (**E1–E3**) The OD value at 450 nm of Jurkat cells post-transfected with miR-410-3p inhibitor or normal control for 24, 48, and 72 h ($n = 4$). For **B–E**, each *dot* represents the average of three repeats from one experiment, and n represents the number of independent experiments done (*$P < 0.05$, **$P < 0.01$, ***$P < 0.001$).

in VKH, Jurkat cells were transfected with miR-410-3p mimics or inhibitor. The transfection efficiency was evaluated using flow cytometry (Fig. 3B), and the relative expression of miR-410-3p in Jurkat cells was found to be significantly higher after transfection with miR-410-3p mimics than NC (Fig. 3C). Jurkat cell proliferation was evaluated by CCK-8 at 24, 48, and 72 hours after transfection. Compared to NC, the proliferation of Jurkat cells was significantly inhibited at 48 and 72 hours after transfection with miR-410-3p mimics (Figs. 3D2, 3D3). A trend of increased cell proliferation was observed 72 hours after transfection with the miR-410-3p inhibitor (Fig. 3E3).

Because Jurkat cells cannot fully simulate human primary T cells and some function analyses cannot be conducted using Jurkat cells,[32] we verified the function of miR-410-3p on human T cells. $CD4^+$ T cells from healthy volunteers were transfected with miR-410-3p mimics or NC with Immunocult human CD3/CD28 T cell activator. The relative expression

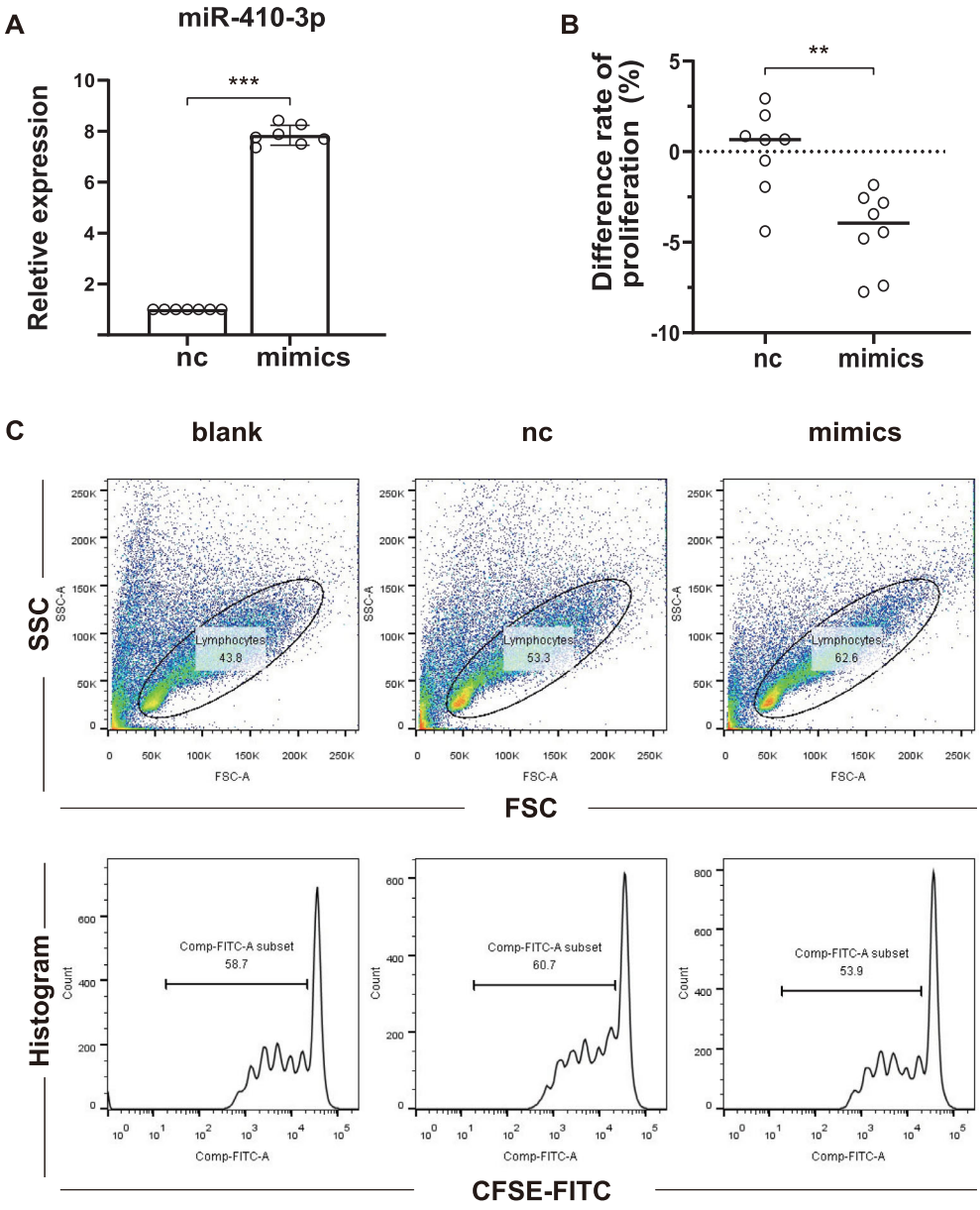

Figure 4. The inhibitory effect of miR-410-3p on the proliferation of $CD4^+$ T cells. (**A**) Relative expression of miR-410-3p in $CD4^+$ T cells was identified using RT-PCR 48 h post-transfected with miR-410-3p mimics or normal control ($n = 7$). (**B**) Histogram of the cell proliferation rate detected by flow cytometry ($n = 8$). (**C**) Representative dot plot and histogram of flow cytometry data. The cell proliferation rate difference between the normal control and mimics was calculated separately using blank as the control. Subsequently, a *t*-test was performed to determine the statistical significance. (*$P < 0.05$, **$P < 0.01$, ***$P < 0.001$).

of miR-410-3p was significantly higher in mimics than NC at 48 hours after transfection (Fig. 4A). The cell proliferation rate in mimics was significantly reduced compared to NC at 96 hours after transfection (Figs. 4B, 4C).

MiR-410-3p Suppressed the T-Cell Proliferation by Downregulating the Expression of CXCL5

The target genes of miRNA-410-3p were predicted using the R package multiMiR (Fig. 5A). KEGG pathway analysis revealed that the target genes of miR-410-3p were mainly associated with the IL-17 and TGF-β signaling pathways, advanced glycation end products-receptor of advanced glycation end products (AGE-RAGE) signaling pathway in diabetic complications, neurotrophin signaling pathway, and cortisol synthesis and secretion (Fig. 5B).

To investigate the target genes of miR-410-3p, the expression levels of the CXCL5 and IFNAR1 genes in Jurkat cells post-transfected with miR-410-3p mimics, inhibitor, or normal control were evaluated. The relative mRNA expression of CXCL5 and IFNAR1 decreased significantly in the mimic-transfected group compared to that in the normal control group (Figs. 6A1, 6A2). The protein expression level of CXCL5 was downregulated in the mimics (Fig. 6B) and upregulated in the inhibitor group, respectively (Fig. 6C). We further tested the role of circulating sEVs in CXCL5

Investigative Ophthalmology & Visual Science

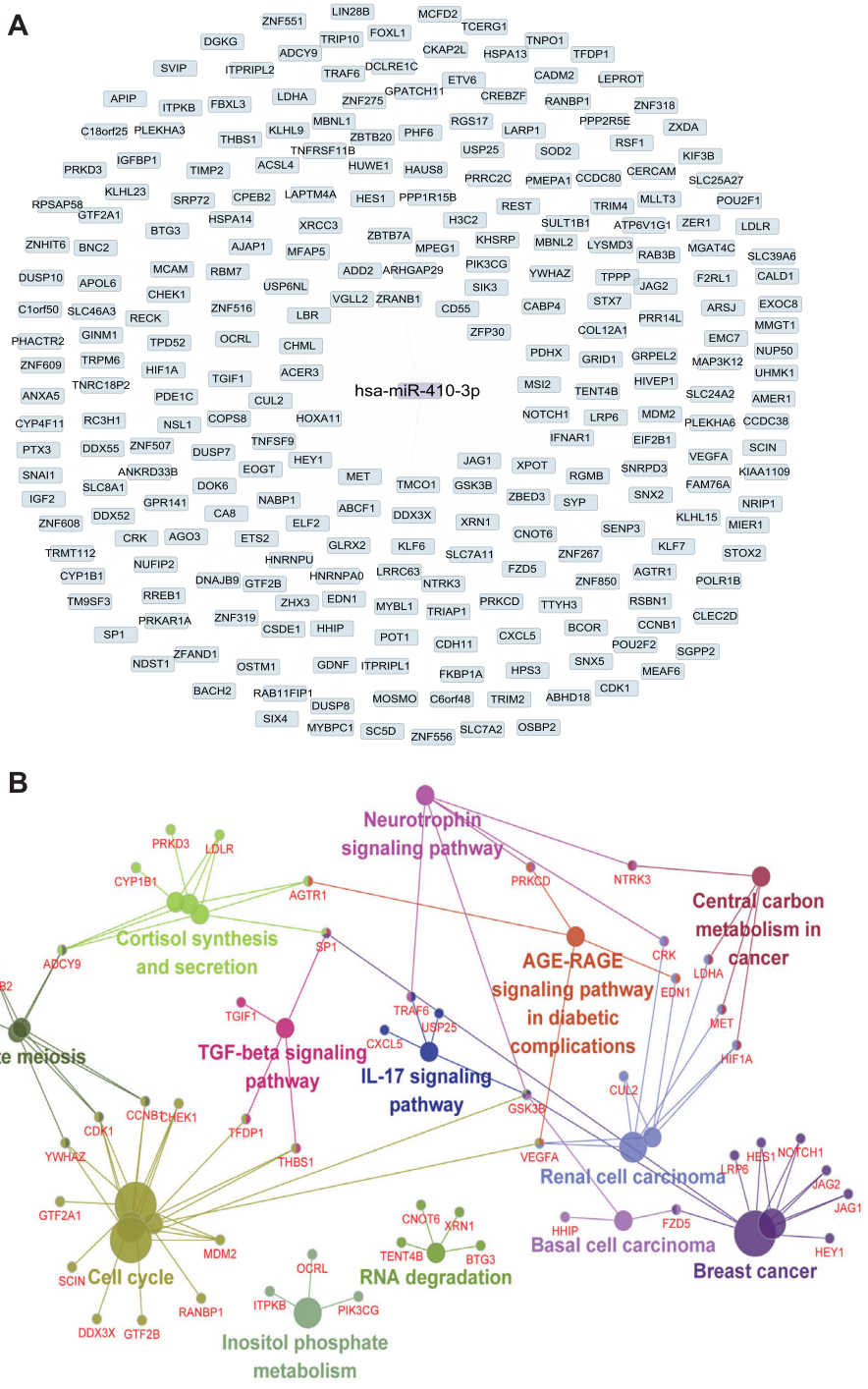

Figure 5. Target gene prediction (**A**) and KEGG pathway analysis (**B**) of miR-410-3p.

expression in $CD4^+$ T cells and confirmed that circulating sEVs derived from patients with VKH could inhibit the expression of CXCL5 in autologous $CD4^+$ T cells (Fig. 6D).

To explore the involvement of CXCL5 in T cell proliferation, Jurkat cells were incubated with increasing doses of exogenous CXCL5. Figure 6E shows that CXCL5 significantly increased the proliferation of Jurkat cells only at 2–10 ng/ml. Jurkat cells were transfected with siRNA to knock down CXCL5, and both the relative mRNA (Fig. 6F) and protein expression (Fig. 6G) of CXCL5 were significantly reduced. Knockdown of CXCL5 with siRNA had an inhibitory effect on Jurkat cell proliferation at 72h (Fig. 6H3). Thus CXCL5 promotes the proliferation of T cells, whereas downregulation of CXCL5 inhibits T cell proliferation. Taken together, these results suggest a specific inhibitory effect of miRNA-410-3p on T cells by suppressing CXCL5 expression, supporting the hypothesis that sEV-derived miRNAs reduce the proliferation of T cells by targeting CXCL5.

Investigative Ophthalmology & Visual Science

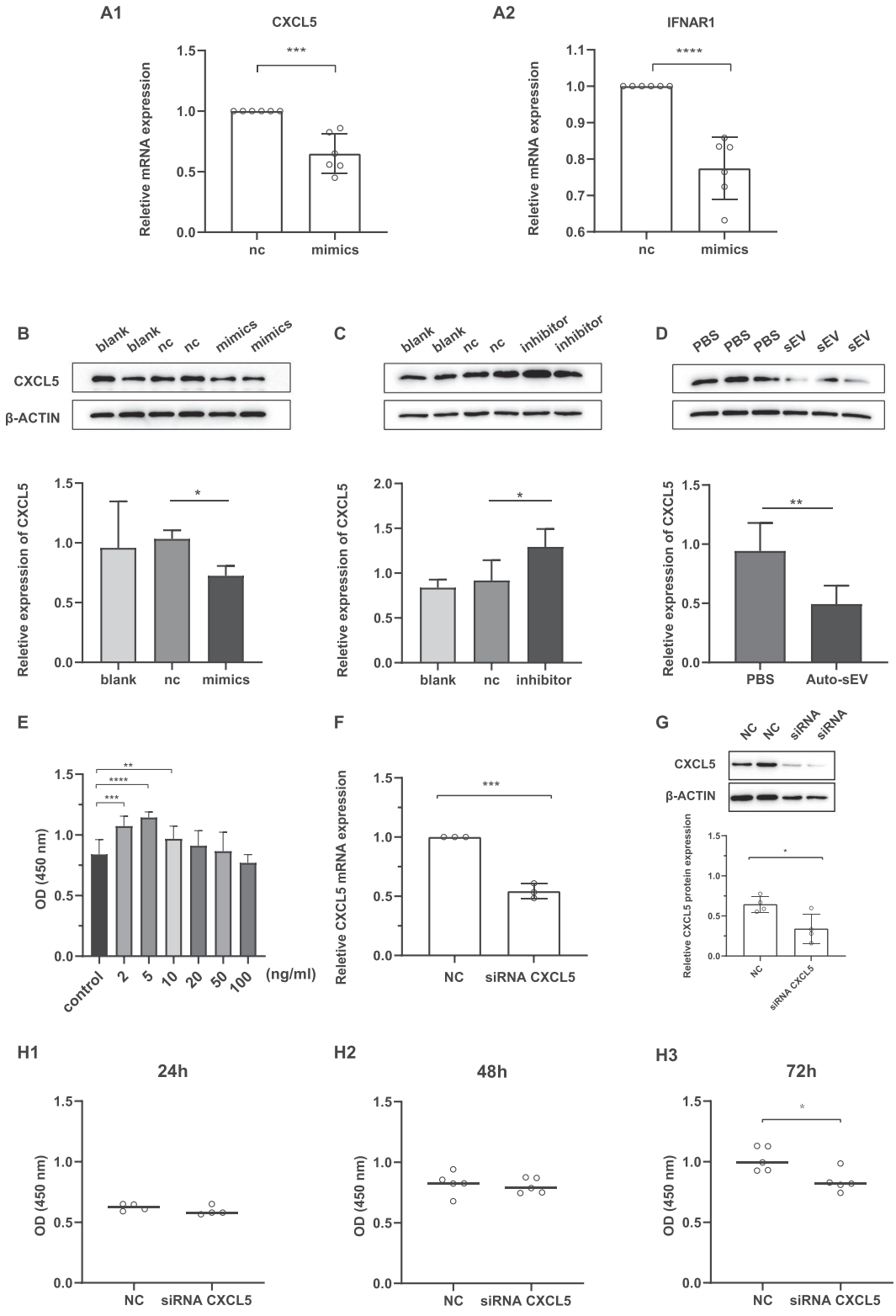

Figure 6. MiR-410-3p suppressed the T cell proliferation by down-regulating the expression of CXCL5. (**A1, A2**) The relative mRNA expression of CXCL5 ($n = 6$) and IFNAR1 ($n = 6$) in Jurkat cells post-transfected with miR-410-3p mimics for 48 hours were measured using RT-PCR. (**B–C**) CXCL5 protein expression in Jurkat cells post-transfected with miR-410-3p mimics or inhibitors measured by Western blotting ($n = 3$). (**D**) CXCL5 protein expression in $CD4^+$ T cells cultured with PBS or with sEVs derived from patients with VKH ($n = 3$), n represents the number of patients. (**E**) Jurkat cells were cultured in a medium supplemented with different concentrations of exogenous CXCL5, then the proliferation of T cells was evaluated by OD value at 450 nm using CCK-8 ($n = 3$). (F-G) Jurkat cells were transfected with siRNA targeting CXCL5, and then cultured for 72 h. The relative expression of CXCL5 mRNA was assessed by RT-PCR (**F**, $n = 3$), and the CXCL5 protein expression was measured by Western blotting (**G**, $n = 4$). (**H1–H3**) The proliferation of Jurkat cells was evaluated by CCK-8 post-transfected with siRNA for 24 h ($n = 4$), 48 h ($n = 5$), and 72 h ($n = 5$). For **A–C** and **E–H**, each *dot* represents the average of three repeats from one experiment, and *n* represents the number of independent experiments performed (*$P < 0.05$, **$P < 0.01$).

Investigative Ophthalmology & Visual Science

Discussion

Exosomes are implicated in the pathogenesis of many autoimmune diseases, such as multiple sclerosis (MS), systemic lupus erythematosus, and autoimmune uveitis.[15,33,34] Circulating exosomes can regulate immune responses and induce immune tolerance in diseases.[35,36] Here we focused on the influence of circulating sEVs on T cells in patients with VKH. We found that circulating sEVs possess immunomodulatory ability in the pathogenesis of VKH, and the encapsulated miRNAs may contribute to the immunosuppressive microenvironment for the induction of immune tolerance.

Plasma-derived circulating sEVs exhibited an antigen-specific inhibitory effect on T cells in a rat model of experimental autoimmune uveitis,[15] whereas vaccination with sEVs in experimental autoimmune uveitis prevents recurrent intraocular inflammation. Here, we confirmed that autologous plasma sEVs could suppress $CD4^+$ T cell proliferation, whereas allogenic sEVs had no such effect. These results suggest that the suppressive effect of circulating sEVs on T cell response is antigen-specific in VKH.

However, the mechanism underlying the immunosuppressive effects of circulating sEVs in VKH has been unclear. MiRNAs can play important roles in T cell–mediated immune responses in autoimmune diseases.[37] MiR-20a-5p was differentially expressed in the $CD4^+$ T cell samples of patients with VKH and could suppress their production of IL-17.[38] MiRNAs are major components of sEV cargoes. We explored the role of miRNAs in circulating sEVs in patients with VKH. We found that among the miRNAs upregulated in sEVs of uveitis with active episodes, miR-410-3p had the largest number of T-cell proliferation target genes, and further experiments confirmed that miR-410-3p could inhibit the proliferation of Jurkat cells, as well as $CD4^+$ T cell. These data suggest a potential function for miR-410-3p in circulating sEVs as a biomarker and suppressive factor in the pathogenesis of VKH. The upregulation of miR-410-3p may contribute to the inhibitory effect of sEVs on $CD4^+$ T-cell proliferation.

The role of MiR-410-3p in cancer and autoimmune diseases is important but controversial and may depend on when it is expressed and which cells express it. MiR-410-3p suppressed tumor cell growth in breast cancer,[39] gliomas,[40] rhabdomyosarcoma,[41] and non-small-cell lung cancer.[42] The expression level of miR-410-3p in synovial tissues and fibroblast-like synoviocytes of rheumatoid arthritis patients were downregulated, and miR-410-3p inhibited inflammatory cytokine secretion[43] and suppressed fibroblast-like synoviocytes proliferation.[44]

We verified that CXCL5 expression was downregulated by miR-410-3p in Jurkat T cells. We found that exogenous CXCL5 promoted the proliferation of Jurkat cells and targeting CXCL5 by siRNA inhibited the proliferation of Jurkat cells in vitro. These results suggest that miR-410-3p may exert a suppressive effect by targeting CXCL5 expression. CXCL5 belongs to the CXC-type chemokine family and participates in inflammatory response by regulating the immune microenvironment.[45,46] It has been shown that CXCL5 plays key roles in promoting cancer cell proliferation, migration, and invasion. Recent studies have shown that CXCL5 may play an important role in autoimmune diseases. It was found that CXCL5 was upregulated in samples of aqueous humor from uveitis patients[47] and the serum of patients with periodontal disease, rheumatoid arthritis,[48] pemphigus vulgaris[49] or moyamoya disease.[50] In relapsing MS patients, the level of CXCL5 in plasma was correlated with the development of new inflammatory lesions, which was considered as a potential novel biomarker and therapeutic target in MS.[51] CXCL5 expression was also elevated in cerebrospinal fluid of MS patients during relapse compared with specimens acquired during remission.[52] Although these reports indicate that CXCL5 may be related to the inflammation state of autoimmune diseases, its effect on T cells is not clear. The present study revealed that CXCL5 could also stimulate the proliferation of T cells, which may promote T-cell–mediated autoimmune responses.

In conclusion, we reported an inhibitory effect of circulating sEVs from VKH on $CD4^+$ T cells mediated by miR-410-3p by targeting CXCL5. Autologous sEVs were used to alleviate T-cell response, which would be a novel, safe, and personalized therapy strategy. Our results indicate that the miR-410-3p/CXCL5 axis may be involved in the pathogenesis of VKH, and miR-410-3p in plasma sEVs may be a useful biomarker for evaluating VKH. This study has a limitation due to a small sample size, and more samples are required to confirm the utility of a biomarker. These results only indicate that autologous sEVs possess the inhibitory effect on $CD4^+$ T cells in patients with VKH. The effect of sEVs from other types of uveitis was not performed and need more experiments in future study. Nevertheless, the role and mechanism of miR-410-3p and CXCL5 in the pathogenesis of VKH are not clear and require additional research.

Acknowledgments

The authors thank Editage (www.editage.cn) for English language editing.

Supported by the National Natural Science Foundation of China (82171042); Natural Science Foundation of Tianjin (20JCZDJC00100); Foundation of Tianjin Key Laboratory of Retinal Functions and Diseases (2019tjswmm002); and Tianjin Key Medical Discipline (Specialty) Construction Project (TJYXZDXK-037A).

Disclosure: **B. Li,** None; **N. Sun,** None; **F. Yang,** None; **K. Guo,** None; **L. Wu,** None; **M. Ma,** None; **H. Shao,** None; **X. Li,** None; **X. Zhang,** None

References

1. Rao NA, Gupta A, Dustin L, et al. Frequency of distinguishing clinical features in Vogt-Koyanagi-Harada disease. *Ophthalmology*. 2010;117:591–599.
2. Wang C, Cao S, Zhang D, Li H, Kijlstra A, Yang P. Increased complement 3a receptor is associated with Behcet's disease and Vogt-Koyanagi-Harada disease. *Sci Rep*. 2017;7:15579.
3. Hou S, Du L, Lei B, et al. Genome-wide association analysis of Vogt-Koyanagi-Harada syndrome identifies two new susceptibility loci at 1p31.2 and 10q21.3. *Nat Genet*. 2014;46:1007–1011.
4. Yoshino N, Kawamura A, Ishii A, et al. Vogt-Koyanagi-Harada disease associated with influenza A virus infection. *Intern Med*. 2018;57:1661–1665.
5. Yang P, Ye Z, Du L, et al. Novel treatment regimen of Vogt-Koyanagi-Harada disease with a reduced dose of corticosteroids combined with immunosuppressive agents. *Curr Eye Res*. 2018;43:254–261.
6. Budmann GA, Franco LG, Pringe A. Long term treatment with infliximab in pediatric Vogt-Koyanagi-Harada disease. *Am J Ophthalmol Case Rep*. 2018;11:139–141.

7. El Andaloussi S, Mäger I, Breakefield XO, Wood MJA. Extracellular vesicles: biology and emerging therapeutic opportunities. *Nat Rev Drug Discov*. 2013;12:347–357.
8. Lawson C, Kovacs D, Finding E, Ulfelder E, Luis-Fuentes V. Extracellular vesicles: evolutionarily conserved mediators of intercellular communication. *Yale J Biol Med*. 2017;90:481–491.
9. Gatti S, Bruno S, Deregibus MC, et al. Microvesicles derived from human adult mesenchymal stem cells protect against ischaemia-reperfusion-induced acute and chronic kidney injury. *Nephrol Dial Transplant*. 2011;26:1474–1483.
10. Del Conde I, Shrimpton CN, Thiagarajan P, López JA. Tissue-factor-bearing microvesicles arise from lipid rafts and fuse with activated platelets to initiate coagulation. *Blood*. 2005;106:1604–1611.
11. Ratajczak J, Miekus K, Kucia M, et al. Embryonic stem cell-derived microvesicles reprogram hematopoietic progenitors: evidence for horizontal transfer of mRNA and protein delivery. *Leukemia*. 2006;20:847–856.
12. Lee Y, El Andaloussi S, Wood MJA. Exosomes and microvesicles: extracellular vesicles for genetic information transfer and gene therapy. *Hum Mol Genet*. 2012;21:R125–R134.
13. Kimura K, Hohjoh H, Fukuoka M, et al. Circulating exosomes suppress the induction of regulatory T cells via let-7i in multiple sclerosis. *Nat Commun*. 2018;9:17.
14. Sun P, Wang N, Zhao P, et al. Circulating exosomes control CD4 T cell immunometabolic functions via the transfer of miR-142 as a novel mediator in myocarditis. *Mol Ther*. 2020;28:2605–2620.
15. Jiang G, Yun J, Kaplan HJ, Zhao Y, Sun D, Shao H. Vaccination with circulating exosomes in autoimmune uveitis prevents recurrent intraocular inflammation. *Clin Exp Ophthalmol*. 2021;49:1069–1077.
16. Sáenz-Cuesta M, Osorio-Querejeta I, Otaegui D. Extracellular vesicles in multiple sclerosis: what are they telling us? *Front Cell Neurosci*. 2014;8:100.
17. Mueller DL. Mechanisms maintaining peripheral tolerance. *Nat Immunol*. 2010;11:21–27.
18. Jung SM, Kim W-U. Targeted Immunotherapy for autoimmune disease. *Immune Netw*. 2022;22:e9.
19. von Boehmer H, Daniel C. Therapeutic opportunities for manipulating T(Reg) cells in autoimmunity and cancer. *Nat Rev Drug Discov*. 2013;12:51–63.
20. Moorman CD, Sohn SJ, Phee H. Emerging therapeutics for immune tolerance: tolerogenic vaccines, T cell therapy, and IL-2 therapy. *Front Immunol*. 2021;12:657768.
21. Théry C, Witwer KW, Aikawa E, et al. Minimal information for studies of extracellular vesicles 2018 (MISEV2018): a position statement of the International Society for Extracellular Vesicles and update of the MISEV2014 guidelines. *J Extracell Vesicles*. 2018;7:1535750.
22. Yang P, Zhong Y, Du L, et al. Development and evaluation of diagnostic criteria for Vogt-Koyanagi-Harada disease. *JAMA Ophthalmol*. 2018;136:1025–1031.
23. Zheng H, Yang F, Ea V, et al. Proteomics profiling of plasma exosomes in VKH patients. *Curr Mol Med*. 2021;21:675–689.
24. Théry C, Amigorena S, Raposo G, Clayton A. Isolation and characterization of exosomes from cell culture supernatants and biological fluids. *Curr Protoc Cell Biol*. 2006;Chapter 3:Unit 3.22.
25. Xiao J, Zhang H, Yang F, et al. Proteomic analysis of plasma sEVs reveals that TNFAIP8 is a new biomarker of cell proliferation in diabetic retinopathy. *J Proteome Res*. 2021;20:1770–1782.
26. Mengjun LG. TCseq: time course sequencing data analysis. 2020;1–8.
27. Ru Y, Kechris KJ, Tabakoff B, et al. The multiMiR R package and database: integration of microRNA-target interactions along with their disease and drug associations. *Nucleic Acids Res*. 2014;42:e133.
28. Yu G, Wang LG, Han Y, He QY. clusterProfiler: an R package for comparing biological themes among gene clusters. *Omics*. 2012;16:284–287.
29. Yu G, He QY. ReactomePA: an R/Bioconductor package for reactome pathway analysis and visualization. *Mol Biosyst*. 2016;12:477–479.
30. Wickham H. *ggplot2: Elegant Graphics for Data Analysis*. New York: Springer-Verlag; 2016.
31. Pompura SL, Dominguez-Villar M. The PI3K/AKT signaling pathway in regulatory T-cell development, stability, and function [published online ahead of print January 22, 2018]. *J Leukocyte Biol*, http://doi.org/10.1002/JLB.2MIR0817-349R.
32. Bloemberg D, Nguyen T, MacLean S, et al. A high-throughput method for characterizing novel chimeric antigen receptors in Jurkat cells. *Mol Ther Methods Clin Dev*. 2020;16:238–254.
33. Kimura K, Hohjoh H, Fukuoka M, et al. Circulating exosomes suppress the induction of regulatory T cells via let-7i in multiple sclerosis. *Nat Commun*. 2018;9:17.
34. Liu D, Zhang N, Zhang X, Qin M, Dong Y, Jin L. MiR-410 Down-regulates the expression of interleukin-10 by targeting STAT3 in the pathogenesis of systemic lupus erythematosus. *Cell Physiol Biochem*. 2016;39:303–315.
35. Ostman S, Taube M, Telemo E. Tolerosome-induced oral tolerance is MHC dependent. *Immunology*. 2005;116:464–476.
36. Kim SH, Bianco NR, Shufesky WJ, Morelli AE, Robbins PD. MHC class II+ exosomes in plasma suppress inflammation in an antigen-specific and Fas ligand/Fas-dependent manner. *J Immunol*. 2007;179:2235–2241.
37. Okoye IS, Coomes SM, Pelly VS, et al. MicroRNA-containing T-regulatory-cell-derived exosomes suppress pathogenic T helper 1 cells. *Immunity*. 2014;41:89–103.
38. Chang R, Yi S, Tan X, et al. MicroRNA-20a-5p suppresses IL-17 production by targeting OSM and CCL1 in patients with Vogt-Koyanagi-Harada disease. *Br J Ophthalmol*. 2018;102:282–290.
39. Zhang Y-F, Yu Y, Song W-Z, et al. MiR-410-3p suppresses breast cancer progression by targeting Snail. *Oncol Rep*. 2016;36:480–486.
40. Wang C, Huang S, Rao S, et al. Decreased expression of miR-410-3p correlates with poor prognosis and tumorigenesis in human glioma. *Cancer Manag Res*. 2019;11:10581–10592.
41. Zhang L, Pang Y, Cui X, et al. MicroRNA-410-3p upregulation suppresses proliferation, invasion and migration, and promotes apoptosis in rhabdomyosarcoma cells. *Oncol Lett*. 2019;18:936–943.
42. Wang H, Feng L, Zheng Y, et al. LINC00680 promotes the progression of non-small cell lung cancer and functions as a sponge of miR-410-3p to enhance HMGB1 expression. *Onco Targets Ther*. 2020;13:8183–8196.
43. Wang Y, Xu N, Zhao S, et al. MiR-410-3p suppresses cytokine release from fibroblast-like synoviocytes by regulating NF-κB signaling in rheumatoid arthritis. *Inflammation*. 2019;42:331–341.
44. Wang Y, Jiao T, Fu W, et al. MiR-410-3p regulates proliferation and apoptosis of fibroblast-like synoviocytes by targeting YY1 in rheumatoid arthritis. *Biomed Pharmacother*. 2019;119:109426.
45. Zlotnik A, Yoshie O. The chemokine superfamily revisited. *Immunity*. 2012;36:705–716.
46. Zhang W, Wang H, Sun M, et al. CXCL5/CXCR2 axis in tumor microenvironment as potential diagnostic biomarker and therapeutic target. *Cancer Commun (Lond)*. 2020;40:69–80.

Investigative Ophthalmology & Visual Science

47. El-Asrar AMA, Berghmans N, Al-Obeidan SA, et al. Differential CXC and CX3C chemokine expression profiles in aqueous humor of patients with specific endogenous uveitic entities. *Invest Ophthalmol Vis Sci*. 2018;59:2222–2228.
48. Panezai J, Ali A, Ghaffar A, et al. Upregulation of circulating inflammatory biomarkers under the influence of periodontal disease in rheumatoid arthritis patients. *Cytokine*. 2020;131:155117.
49. Fujimura T, Kakizaki A, Furudate S, Aiba S. A possible interaction between periostin and CD163 skin-resident macrophages in pemphigus vulgaris and bullous pemphigoid. *Exp Dermatol*. 2017;26:1193–1198.
50. Fujimura M, Fujimura T, Kakizaki A, et al. Increased serum production of soluble CD163 and CXCL5 in patients with moyamoya disease: involvement of intrinsic immune reaction in its pathogenesis. *Brain Res*. 2018;1679:39–44.
51. Rumble JM, Huber AK, Krishnamoorthy G, et al. Neutrophil-related factors as biomarkers in EAE and MS. *J Exp Med*. 2015;212:23–35.
52. Blackmore S, Hernandez J, Juda M, et al. Influenza infection triggers disease in a genetic model of experimental autoimmune encephalomyelitis. *Proc Natl Acad Sci USA*. 2017;114:E6107–E6116.

Investigative Ophthalmology & Visual Science